*Sample Collection and RNA Extraction*

Tumor specimens for molecular genetic analysis were obtained from 29 patients with meningioma and 25 patients with high-grade glioma who underwent surgical procedures at Nagoya University Hospital or affiliated hospitals. The molecular genetic analysis performed in this study was approved by the institutional ethics committee of Nagoya University, and all patients who registered for this study provided written informed consent. All tumors were histologically verified according to the WHO 2007 guidelines; 23 patients had grade-I meningioma, 5 had grade-II meningioma, 1 had grade-III meningioma, 6 had grade-III glioma, and 19 had grade-IV glioma. RNA purification was performed using the standard TRIzol (Invitrogen, Carlsbad, CA) method.

*Quantitative Analysis of WT1 mRNA Expression*

Total RNA was extracted from 54 tumors, 3 cell lines, and normal whole brain (Human Total RNA Master Panel II; Takara Bio, Otsu, Japan), and first-strand cDNA was synthesized using the Transcriptor First Strand cDNA Synthesis Kit (Roche, Mannheim, Germany). The cDNA product was used in reverse-transcription (RT) PCR for the quantitation of *WT1* and *GAPDH* mRNA levels. The primers and Taqman probes for the assay were purchased from Roche Diagnostics (Indianapolis, IN). The sequences of the primers and probe used to detect *WT1* mRNA were as follows: WT1 forward primer (5′-GATAACCACAC AACGCCCATC-3′), WT1 reverse primer (5′-CACACG TCGCACATCCTGAAT-3′), and WT1 probe (5′-FAM-ACACCGTGCGTGTGTATTCTGTATTGG-TAMRA-3′). The sequences of the primers used to detect *GAPDH* mRNA were as follows: GAPDH forward primer (5′-AGCCA CATCGCTCAGACAC-3′) and GAPDH reverse primer (5′-GCCCAATACGACCAAATCC-3′). The GAPDH probe was from the Roche Human Probe Library (no. 60). RT-PCR assay was performed using the LightCycler 480 Probes Master and LightCycler 480 instrument II (Roche Diagnostics). *WT1* expression was normalized to that of *GAPDH* in each sample.

*Measurement of Proviral Copy Number in Retrovirus-Transduced PBMCs*

Genomic DNA was purified from transduced PBMCs, and the mean proviral copy number per cell was quantified using the Cycleave PCR core kit (Takara Bio) and Proviral Copy Number Detection Primer Set (Takara Bio).

*Flow Cytometry*

PE-conjugated anti-human CD4 monoclonal antibody (mAb; eBioscience, San Diego, CA), FITC-conjugated anti-human CD8 mAb (BD Biosciences, San Diego, CA), and PE-conjugated $WT1_{235-243}$/HLA-A*2402 tetramer (provided by Dr. Kuzushima, Aichi Cancer Center Research Institute) were used. Stained cells were analyzed using a FACScanto II flow cytometer (BD Biosciences).

For intracellular IFN-γ staining, PBMCs ($1.0 \times 10^6$ cells) were cultured with IOMM-Lee or KT21-MG1 meningioma cells ($1.0 \times 10^6$ cells) for 1 h. BD GolgiStop (0.7 μg/mL; BD Biosciences) was added, and cells were cultured for an additional 8 h. Then, the PBMCs were incubated with Fc blocker (eBioscience, San Diego, CA) and stained with FITC-conjugated anti-human CD8 mAb. After this, the PBMCs were incubated with BD Cytofix/Cytoperm solution (BD Biosciences) at 4°C for 20 min and then washed with BD Perm/Wash solution (BD Biosciences). The PBMCs were then incubated with APC-conjugated anti-human IFN-γ mAb (BD Biosciences), followed by flow cytometry.

*Calcein-AM Cytotoxicity Assay*

The ability of the transduced PBMCs to lyse target cells was measured using a calcein-AM (Dojindo, Kumamoto, Japan) release assay, as described previously.[22] In brief, $5 \times 10^3$ calcein-AM–labeled target cells and various numbers of effector cells in 200 μL of RPMI 1640 medium containing 10% fetal bovine serum were seeded into 96-well round-bottom plates. The target cells were incubated with or without 10 nM WT1 peptide for 2 h before the addition of effector cells. After incubation with the effector cells for 4 h, 100 μL of supernatant was collected from each well. The percentage of specific lysis was calculated according to the formula [(experimental release – spontaneous release)/(maximum release – spontaneous release)] × 100.

*Generation of Green Fluorescent Protein–Expressing IOMM-Lee Cells*

A retrovirus expressing green fluorescent protein (GFP) was constructed using the Retro-X Universal Packaging System (Clontech, CA). GP2-293 cells were transfected with pRetroQ-AcGFP-C1 along with a pVSVG plasmid (Clontech). After 48 h, cell-free viral supernatants were obtained and stored at −80°C. IOMM-Lee cells were transduced with the retroviral vectors encoding GFP with use of the RetroNectin-bound Virus Infection Method, in which retroviral solutions were preloaded onto RetroNectin-coated plates, centrifuged at 2000 × *g* for 2 h, and rinsed with PBS. IOMM-Lee cells were then applied onto the preloaded plate.

*Skull Base Meningioma Xenograft*

NOD/Shi-SCID, IL-2R$\gamma_c^{null}$ (NOG) mice were created at the Central Institute of Experimental Animals (Kawasaki, Japan) by backcrossing $\gamma_c^{null}$ mice with NOD/Shi-SCID mice, as reported previously.[23] Eight-week-old mice were given intracranial injections containing 3 μL of $5.0 \times 10^4$ freshly dissociated GFP-expressing IOMM-Lee cells with use of the PGFi technique.[24] In brief, the mice were anesthetized with

an intraperitoneal injection of 45 mg/kg sodium pentobarbital (Dainippon Sumitomo Pharma, Osaka, Japan). A 26-gauge needle tip was positioned on the right PGF (the rostral area of the opening of the external acoustic meatus). The implantation site, the lateral part of the foramen ovale, was accessed via the following injection track: horizontal angle, 60°; sagittal angle, −45°; and insertion depth, 3 mm (Supplementary Material, Fig. S1A and B). The cells were injected over 5 s. The needle was slowly withdrawn over several seconds. Minimal finger pressure was applied for 30 s after needle withdrawal to stop the bleeding at the puncture site. After the injections, the mice were given free access to water and were examined twice per day. Corneal sensitivity was also recorded using a cotton filament, and the blinking of the right eye was compared with that of the control (left) eye.

### *In Vivo Anti-Meningioma Effects of WT1-siTCR Gene-Transduced CTLs*

In our preliminary experiments, the median survival of untreated animals was consistently 12.5 days (data not shown). Twenty-four mice bearing established tumors were randomly assigned to 2 different experimental groups. Five days after tumor inoculation, human PBMCs ($5.0 \times 10^7$ cells) were injected into the tail vein. On the twelfth day after tumor inoculation, 6 mice per group were sacrificed to evaluate tumor size and $CD8^+$ T cell infiltration. According to statistical considerations based on our preliminary experiments, the remaining mice were monitored for signs of keratopathy and survival for up to 28 days after inoculation,

### *Tissue Processing and Immunohistochemistry*

Mouse heads were fixed in 10% neutral buffered formalin (Wako Pure Chemical Industries, Osaka, Japan) for 48 h. GFP fluorescence in tumor cells was analyzed using a fluorescence imaging system (IVIS spectrum; Caliper Life Sciences, Alameda, CA) after the removal of the skull. Two-dimensional tumor size was calculated from the fluorescent area by using the Living Image software (Caliper Life Sciences), because the established tumors grew in a flattened pattern, similar to meningioma en plaque in humans. For histopathologic examination, formalin-fixed mouse heads were decalcified in Decalcifying Solution B (Wako Pure Chemical Industries) for 96 h and embedded in paraffin. Serial 5-μm sections were cut and processed for hematoxylin and eosin (H&E) staining, Luxol fast blue (LFB) staining, or immunohistochemistry. The sections were deparaffinized with xylene and rehydrated with ethanol. LFB staining was performed according to the method of Werner et al.[25] In brief, the sections were placed in 0.1% LFB solution at 60°C for 16 h. After several washes, sections were differentiated in 0.05% lithium carbonate solution, followed by 70% ethanol. The slides were then incubated in 0.1% Cresyl echt violet solution to counterstain nuclei. Immunohistochemistry for human $CD8^+$ T cells was performed using anti-human CD8 antibody (MBL, Nagoya, Japan). In brief, the sections were rinsed in PBS and incubated with the antibody freshly diluted at 1:100 in PBS. The Vector M.O.M. Immunodetection Kit (Vector Laboratories, Burlingame, CA) was used to perform the secondary antibody incubations. The staining was visualized with diaminobenzidine, and sections were counterstained with hematoxylin. We counted the number of both normal tissue-infiltrating (oral mucosa and submucosal soft tissues) and tumor-infiltrating $CD8^+$ T cells in a microscopic grid 0.5 × 0.5 mm in size (0.25 $mm^2$) at a magnification of 200×. The area with the most abundant distribution of $CD8^+$ T cells was selected in each mouse.

### *Statistical Analysis*

Comparisons between groups were done using paired *t* test or Welch's *t* test or Mann–Whitney exact test, where appropriate. Differences were considered to be statistically significant at $P < .05$. The outliers were defined as data points that were >3 times the interquartile ranges below the first quartile or above the third quartile. The Kaplan-Meier method and log-rank test were used to determine whether there was a significant difference in clinical events between the groups.

## Results

### WT1 *Expression in Meningioma Patient Samples and Cell Lines*

*WT1* mRNA levels in samples from patients with meningioma and human meningioma cell lines were determined using quantitative RT-PCR and calculated relative to the WT1 expression level in the normal brain. As shown in Table 1, *WT1* mRNA was expressed at high levels in samples from patients with meningioma. Of interest, a correlation was found between the *WT1* expression levels and the MIB-1 labeling index ($P = .0018$, Fig. 1A), but there was no significant correlation with tumor location, tumor grading, and performance status (modified Rankin scale). We also examined *WT1* expression in 25 high-grade glioma samples. The mean expression level of *WT1* mRNA in meningioma samples was significantly higher than that in high-grade glioma samples (26.25 [18.27] vs. 5.45 [12.52]; $P = .000014$). The genotype, *WT1* expression levels, and intracranial tumorigenicity of NOG mice implanted with the 3 meningioma cell lines are presented in Table 2. In all the 3 meningioma cell lines, the *WT1* mRNA levels were >8-fold higher than that of the normal brain.

### *Cell Surface Expression of CD4, CD8, and WT1-Specific TCR in NGMCs and GMCs*

PBMCs were transduced with WT1-siTCR at relatively low copy numbers to reduce the risk of insertional

**Table 1.** Data on patients with meningiomas and tumor characteristics

| | Age (years)/ Sex | Location of Lesion | Pathological Diagnosis (subtype) | WHO Grade | MIB-1 Index (%) | Relative Quantity of WT1 mRNA (NB = 1) | Extent of Resection (Simpson grade) | Follow-up Period (month) | Recurrence/ Regrowth | mRS |
|---|---|---|---|---|---|---|---|---|---|---|
| 1 | 71M | SB | meningothelial | I | ND | 19.43 | 2 | 39 | − | 0 |
| 2 | 49F | non- SB | meningothelial | I | ND | 5.06 | 2 | 55 | − | 0 |
| 3 | 69F | non- SB | fibrous | I | ND | 27.86 | 3 | 77 | − | 0 |
| 4 | 68F | non- SB | transitional | I | ND | 22.78 | 1 | 77 | − | 0 |
| 5 | 30F | SB | meningothelial | I | ND | 25.63 | 2 | 23 | − | 1 |
| 6 | 68M | SB | meningothelial | I | ND | 12.64 | 4 | 15 | − | 5 |
| 7 | 73F | SB | meningothelial | I | ND | 20.68 | 2 | 32 | − | 1 |
| 8 | 46F | SB | meningothelial | I | <1 | 7.78 | 2 | 76 | − | 0 |
| 9 | 36F | SB | meningothelial | I | ND | 22.63 | 2 | 65 | − | 1 |
| 10 | 64M | SB | meningothelial | I | ND | 12.55 | 2 | 7 | − | 2 |
| 11 | 56M | non- SB | fibrous | I | ND | 48.17 | 1 | 57 | − | 0 |
| 12 | 46F | non- SB | meningothelial | I | ND | 56.89 | 1 | 69 | − | 0 |
| 13 | 42F | non-s SB | meningothelial | I | ND | 4.50 | 1 | 89 | − | 2 |
| 14 | 58M | SB | meningothelial | I | 5 | 38.59 | 2 | 65 | + | 1 |
| 15 | 39F | non- SB | transitional | I | 3 | 39.67 | 1 | 2 | − | 3 |
| 16 | 72F | non- SB | fibrous | II | 3 | 33.13 | 2 | 72 | + | 1 |
| 17 | 63M | SB | atypical | II | 4 | 60.97 | 4 | 63 | − | 1 |
| 18 | 77M | SB | meningothelial | I | 1–2 | 4.03 | 4 | 70 | − | 0 |
| 19 | 54M | SB | meningothelial | I | 1–3 | 7.57 | 4 | 53 | − | 2 |
| 20 | 33F | non- SB | meningothelial | II | 5–6 | 47.50 | 4 | 16 | − | 2 |
| 21 | 48F | SB | meningothelial | I | ND | 28.25 | 2 | 57 | − | 1 |
| 22 | 62M | SB | meningothelial | I | ND | 47.84 | 4 | 2 | − | 1 |
| 23 | 66F | SB | meningothelial | II | ND | 58.49 | 1 | 48 | − | 2 |
| 24 | 70F | SB | atypical | II | 20–30 | 41.64 | 2 | 80 | + | 1 |
| 25 | 52M | SB | atypical | II | 10–15 | 14.22 | 3 | 37 | + | 5 |
| 26 | 55M | SB | atypical | II | 2 | 4.63 | 2 | 73 | − | 1 |
| 27 | 63M | non- SB | atypical | II | 4 | 2.79 | 2 | 83 | − | 0 |
| 28 | 45M | non- SB | clear cell | II | 1–2 | 9.06 | 1 | 92 | − | 0 |
| 29 | 68F | non- SB | anaplastic | III | 3–10 | 36.25 | 3 | 64 | + | 2 |

Abbreviations: mRS, modified Rankin Scale; NB, normal brain; ND, not done; SB, skull base.

mutagenesis. In the GMCs used in this study, the proviral copy number was 2.24 copies per cell (data not shown). $CD4^+$ and $CD8^+$ cells constituted 14.6% and 78.4% of NGMCs and 19.7% and 72.8% of GMCs, respectively (Fig. 1B). About 20% of the GMCs were positive for HLA-A*2402/WT1 tetramer staining (Fig. 1B). Moreover, HLA-A*2402/WT1-tetramer positivity in $CD3^+CD8^+$ cells and $CD3^+CD4^+$ cells was 36.2% and 36.3%, respectively, suggesting that both fractions were similarly transduced (Supplementary Material, Fig. S3A). These NGMCs and GMCs were used as effector cells in subsequent assays.

### *Intracellular IFN-γ Production by GMCs Against Human Meningioma Cell Lines*

To confirm that the freezing and thawing procedures had not affected the antigen specificity and HLA restriction of GMCs, we first investigated their intracellular IFN-γ production in response to WT1-peptide–loaded and nonloaded T2A24 cells. As demonstrated previously, GMCs exhibited specific reactivity to WT1-peptide–pulsed T2A24 cells (data not shown).[4,5] We also investigated the intracellular IFN-γ production in NGMCs and GMCs against WT1-positive meningioma cell lines, KT21-MG1 (HLA-A*2402 negative) and IOMM-Lee (HLA-A*2402 positive). As shown in Fig. 1C, GMCs exhibited specific reactivity to IOMM-Lee cells. These data confirm that GMCs can recognize WT1-positive meningioma cells in an HLA-A*2402–restricted manner.

### *Cytotoxicity of GMCs Against Human Meningioma Cell Lines*

To determine whether GMCs were able to lyse target cells, effector cells were mixed with calcein-AM–labeled target cells. As shown in Fig. 1D, GMCs lysed

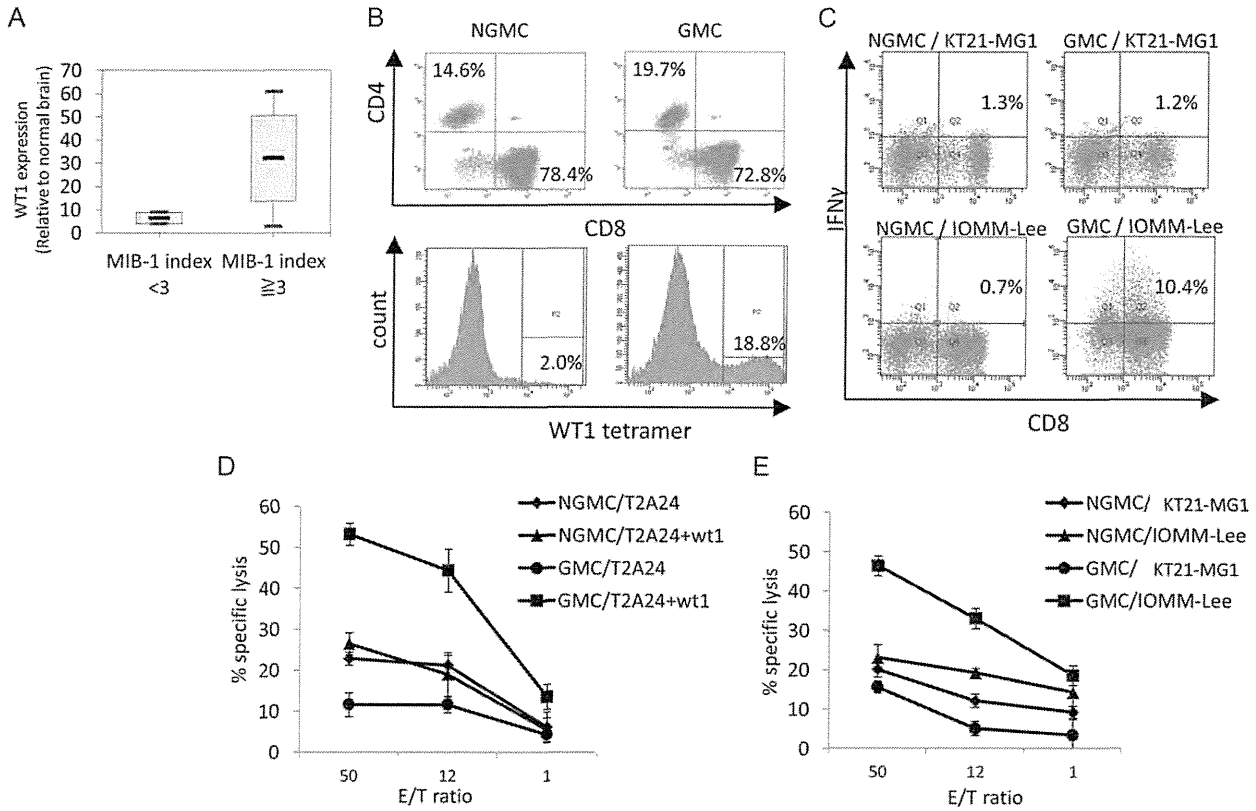


Fig. 1. Correlation between Wilms' tumor protein (WT1) expression and MIB-1 index (A) in vitro effector activity of Wilms' tumor protein (WT1)–targeted peripheral blood mononuclear cells (PBMCs). Gene-modified PBMCs (GMCs) were produced by transducing PBMCs with the WT1-siTCR vector. Non–gene-modified PBMCs (NGMCs) were used as a negative control. (B) $CD4^+$ and $CD8^+$ cells constitute 14.6% and 78.4% of NGMCs and 19.7% and 72.8% of GMCs, respectively. The proportions of WT1-tetramer–positive cells in NGMCs and GMCs are shown in the lower column. (C) Intracellular interferon-γ (IFN-γ) production by NGMCs and GMCs against human meningioma cell lines. NGMCs and GMCs were cocultured with WT1-positive and HLA-A*2402–negative KT21-MG1 cells or WT1-positive and HLA-A*2402–positive IOMM-Lee cells. The PBMCs were analyzed for intracellular IFN-γ production. (D and E) WT1-specific and HLA-A*2402–restricted cytotoxicity of GMCs. Cytotoxic activities of NGMCs and GMCs against WT1-peptide–loaded and nonloaded T2A24 cells (D) and KT21-MG1 and IOMM-Lee cells (E) were examined using the calcein-AM assay at various effector/target (E/T) ratios.

**Table 2.** Characteristics of human meningioma cell lines

| Cell Line | Relative Quantity of WT1 mRNA (NB = 1) | HLA-A Genotyping | Intracranial Tumorigenicity in Immunocompromised Mice |
|---|---|---|---|
| HKBMM | 8.51 | 2402/1101 | − |
| IOMM-Lee | 8.82 | 2402/0301 | + |
| KT21-MG1 | 18.77 | 0207/1101 | − |

Abbreviation: NB, normal brain.

T2A24 cells that had been loaded with the WT1-peptide, but were not cytotoxic against nonloaded cells. The cytotoxicities of GMCs against human meningioma cell lines are shown in Fig. 1E. GMCs exhibited significant lytic activity against IOMM-Lee cells but not KT21-MG1 cells. These results strongly suggest that WT1-specific effector cells can lyse meningioma cells via recognition of their WT1-derived peptide in the context of HLA-A*2402.

### *Establishment of a Mouse Model of Skull Base Meningioma*

Recently, we developed PGFi, a simple method that enables percutaneous injection of cells into the mouse brain. Because the PGFi technique provides access to the skull base area with minimal brain damage from needle penetration, we applied this technique to establish a mouse model of skull base meningioma. We selected the lateral part of the right foramen ovale as a tumor implantation site and used the needle trajectory shown in Supplementary Material, Fig. S1. GFP-labeled IOMM-Lee cells (IOMM-Lee-GFP) were implanted into 9 NOG mice. At 5 and 10 days after xenografting, 3 mice each were sacrificed and tumor growth was assessed. On day 14, the remaining 3 mice appeared to be sickly, and they were sacrificed for the assessment of tumor size. The overall intraoperative mortality was 0%, with a tumor induction rate of 100%. Representative macroscopic pictures, fluorescence images, and the corresponding H&E-stained sections

of the IOMM-Lee-GFP skull base xenografts are shown in Fig. 2A. Tumors were induced in the right temporal fossa, enlarged rapidly and encased the ipsilateral trigeminal nerves, and extended into the contralateral skull base in the late phase. Macroscopic analysis revealed that tumors grew along the skull base and did not invade the surface of the brain (Fig. 2B). Because tumors grew in a flattened pattern, we used the 2-dimensional tumor size, which was calculated from the fluorescent area, to assess the tumor size. Fig. 2C shows the line graph representing the mean tumor size on days 5, 10, and 14 after implantation. Clinical monitoring of tumor-bearing mice revealed progressive ophthalmic signs, including decreased blink reflex and corneal aberration (Fig. 3A). These signs were consistent with a diagnosis of neurotrophic keratopathy. It is known that the trigeminal nerve provides corneal innervations, and corneal denervation abolishes the corneal blink reflex and leads to neurotrophic keratopathy. In a previous study on a mouse model of neurotrophic keratopathy, Ferrari et al damaged the mouse's trigeminal nerve at the skull base by electrolysis to induce ipsilateral neurotrophic keratopathy.[26] They reported that electrode insertion did not cause keratopathy and that electrocoagulation was required to induce keratopathy. Similarly, no keratopathy was caused by needle insertion alone in our model, because the needle was inserted to the skull base just lateral to the foramen ovale (Supplementary Material, Fig. S1). We performed histopathologic analysis on the symptomatic mice. The right trigeminal nerves were encased and infiltrated by tumor cells and exhibited extensive disruption compared with the contralateral nerves (Fig. 3B). Thus, in our mouse model, keratopathy was considered to be caused by skull base meningioma, and it provided an indirect indication of trigeminal nerve damage caused by the tumor.

### *Effects of GMCs on WT1-Expressing Meningioma In Vivo*

We used our newly developed skull base meningioma model to evaluate the in vivo efficacy of GMCs. Five days after intracranial injection of IOMM-Lee-GFP cells, NGMCs or GMCs were adoptively transferred via the tail vein. Although complete tumor eradication was not observed on day 12, tumor growth was significantly retarded in GMC-injected mice, compared with the control group ($P = .0062$; Fig. 4A–C). In both groups, we counted the number of infiltrating $CD8^+$ T cells in the tumor and normal mesectoderm tissues, including the oral mucosa and submucosal soft tissues (Fig. 4D–F). There was no significant difference in the number of $CD8^+$ T cells infiltrating the normal tissue in the 2 groups. In contrast, the number of $CD8^+$ T cells infiltrating the tumor was greater in the GMC-treated group than in the NGMC-treated group ($P = .0040$). The number of $CD4^+$ T cells infiltrating the normal tissue and the tumor was limited in both the NGMC- and GMC-treated groups (Supplementary Material, Fig. S3B). Moreover, the survival time was remarkably prolonged in GMC-treated mice (log rank test, $P = .0055$; Fig. 5A). Although there were no survivors among the NGMC-treated mice, there were 3 survivors (50%) among the GMC-treated mice by day 28. However, all 3 survivors on day 28 harbored a small size of tumor (Fig. 5B). Consistent with the tumor growth retardation, GMCs decreased the incidence and delayed the onset of neurotrophic keratopathy during the observation period ($P = .014$; Fig. 5C). Two GMC-treated mice (33%) survived with no symptoms of keratopathy until the experiment was terminated at day 28 after tumor inoculation. Therefore, these 2 mice were excluded from the statistical analysis of time to onset.

## Discussion

The principal findings of this study are (1) WT1 is highly expressed in menigiomas and (2) unmanageable skull base meningiomas are markedly treated with adoptive transfer of T cells retrovirally transduced with WT1-specific TCR gene that were also designed to prevent miscoupling with endogenous TCR.

### *WT1-Targeted Cell Therapy*

We investigated the use of WT1 as a target for meningioma immunotherapy. To date, there have been no reports on the relationship between WT1 and meningioma. In the present study, we observed high levels of *WT1* mRNA in meningioma tissues and cultured cell lines. WT1 is highly expressed in various types of tumors, and clinical trials in WT1-targeted immunotherapy have confirmed the safety and clinical efficacy of major histocompatibility complex class I–restricted WT1 epitope peptides.[27,28] Of note, in a recent study, WT1 was selected from 75 defined tumor antigens as the most promising antigen.[29]

Immunotherapy is a conceptually attractive approach for malignant skull base meningioma, because it is highly specific and can deal with adherent and invasive tumor cells with minimal impact on normal vital brain structures. Induction of tumor-specific effector T cells is critical for eradicating bulky solid tumors, and it is the final goal of tumor immunotherapy approaches. Tumor-specific cytotoxic T cells can be genetically engineered to express altered or totally artificial TCRs, but the limited efficacy of TCR gene therapy has been reported to be associated with insufficient surface expression of the transduced TCRs.[30–33] The existence of endogenous TCR is one of the major reasons for this insufficient cell surface expression, because endogenous TCRs compete with the introduced TCRs for CD3 molecules, and the endogenous TCR chains have been reported to mispair with the transduced TCR chains.[33–37] To address this problem, our group has previously constructed a number of siRNAs to knock down the endogenous TCR $\alpha$ and $\beta$ chains, and we have measured the knock-down efficiency. We used a tetramer assay to show that the vector knocking down the endogenous

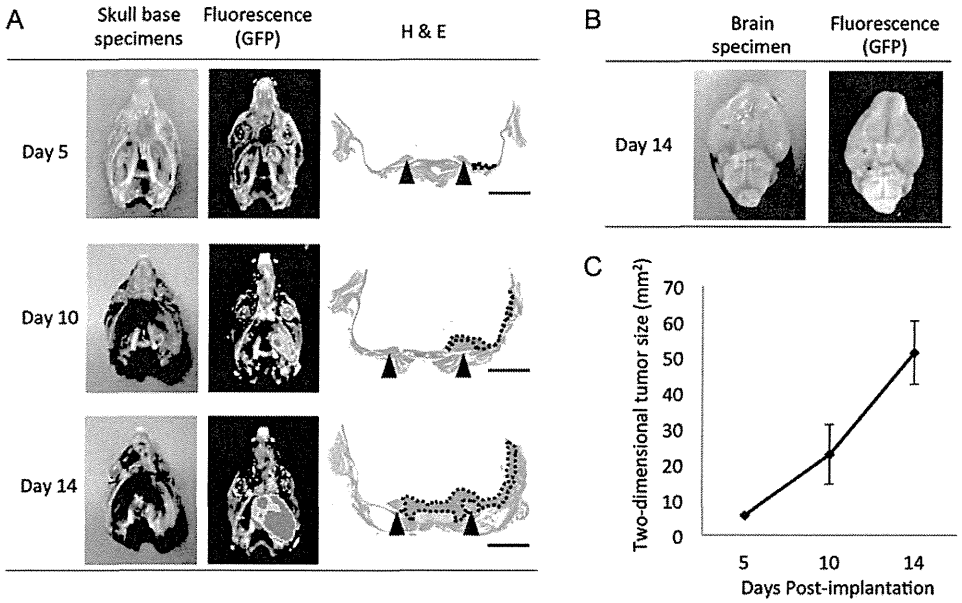


Fig. 2. Representative histologic images of skull base tumor formation at days 5, 10, and 14. (A) White-light imaging, fluorescence imaging, and the corresponding H&E staining of the tumors are shown. The tumor formed from the implanted IOMM-Lee tumor cells labeled with green fluorescent protein (GFP) is seen in the right skull base. Green light emitted from the GFP was captured by a charge-coupled device camera. After fluorescence imaging, the skull base specimens were processed for H&E staining. Scale bar = 2 mm. (B) White-light imaging and fluorescence imaging of the whole brain of a tumor-bearing mouse at day 14. (C) Line graph representing the mean tumor size on days 5, 10, and 14 after tumor implantation.

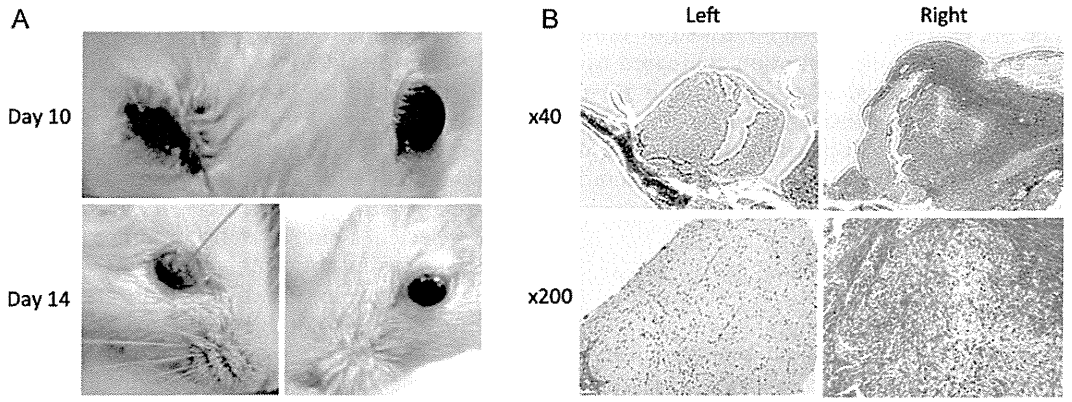


Fig. 3. Skull base meningioma xenograft induces neurotrophic keratopathy by damaging the trigeminal nerve. (A) Representative photographs of the face of a mouse demonstrating the development of neurotrophic keratopathy in the right eye at days 10 and 14 after tumor inoculation in the right skull base. (B) Representative Luxol fast blue staining of the trigeminal nerves of a skull base meningioma-bearing mouse. The right trigeminal nerve is encased and infiltrated by tumor cells and exhibits extensive disruption, compared with the contralateral side. Original magnification: 40× (upper) and 200× (lower).

TCRs most efficiently achieved the highest expression of engineered WT1-TCR.[4] We have also shown that the introduction of WT1-siTCR to HBZ-specific CTLs resulted in an upregulation of WT1-TCR and a downregulation of HBZ-TCR.[5] Using this retroviral vector system, we transduced PBMCs with the HLA-A*2402–restricted and WT1-specific TCR. In a recent preclinical study, Ochi et al reported marked antileukemic reactivity and safety of WT-siTCR–transduced T cells.[5] In the present study, we purposely used PBMCs transduced with WT1-siTCR at relatively low copy numbers with a view to clinical application, because restricting the copy number per cell is ideal for reducing the risk of insertional mutagenesis.[38,39] We first demonstrated that GMCs exhibited a strong cytotoxic effect against human meningioma cells in an HLA-class I–restricted manner. Then, we investigated the in vivo efficacy of a single injection of GMCs. Although complete tumor eradication was not observed, GMCs significantly retarded tumor growth and prolonged the overall

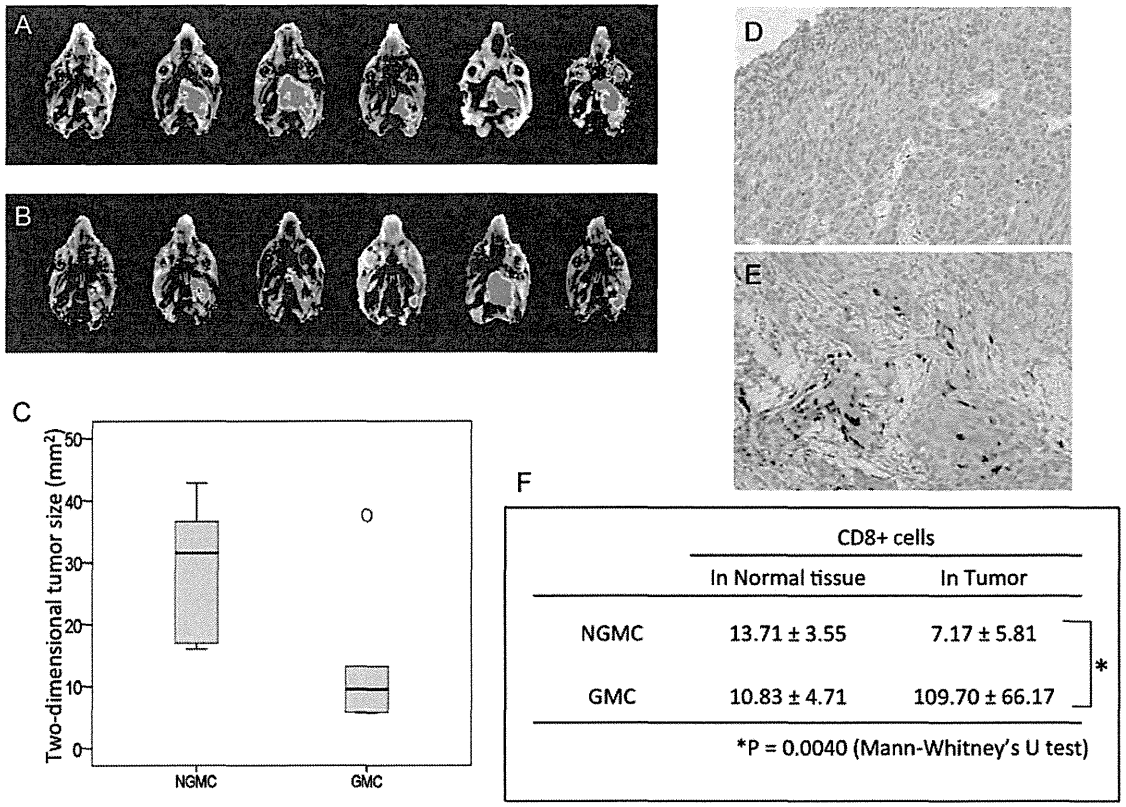


Fig. 4. Inhibition of skull base meningioma growth in NOG mice after adoptive transfer of GMCs. (A and B) Fluorescence images of skull base meningiomas in mice treated with NGMCs (A) and GMCs (B). The lower graph (C) is a summary of the 2-dimensional tumor size in mice treated with NGMCs and GMCs. The black line in the box indicates the median and the open circle indicates the outlier. (D and E) Representative photomicrographs of immunohistochemical staining (human $CD8^+$ T cells) of tumors from NGMC-treated mouse (D) and GMC-treated mouse (E). Original magnification: 200×. The lower table (F) is a summary of normal tissue- and tumor-infiltrating $CD8^+$ T cell counts in mice treated with NGMCs and GMCs.

survival of treated mice. Moreover, GMC treatment significantly retarded the progression of trigeminal nerve damage caused by meningioma. Immunohistochemistry revealed robust accumulation of human $CD8^+$ cells in meningioma lesions, which is a critical factor governing the success of tumor immunotherapy. Our results suggest that gene immunotherapy using WT1-siTCR is a promising new modality for the treatment of difficult-to-treat meningiomas. Before translating the proposed project into a clinical trial, off-target effects on normal tissues are major concerns. We have previously reported that WT1-siTCR CTLs had no cytolytic effects on $CD34^+$ cells.[5] These issues should be addressed in a phase I clinical trial.

### *A Novel Skull Base Meningioma Model*

In addition to the intrinsic biology of meningiomas, tumor location is also an important factor in determining the outcome in patients with meningioma. Skull base is one of the most common locations for meningiomas. Resection of skull base meningiomas can lead to high rates of morbidity and mortality because of their deep locations and the possible involvement of vital brain structures, such as cranial nerves. Cranial nerves arise directly from the brain and are so delicate as to be susceptible to damage by surgical procedures or radiation. Meningiomas have a tendency to involve and infiltrate cranial nerves.[15] It is very difficult to preserve the anatomical and functional integrity of the cranial nerves involved in tumors, particularly in hard lesions, such as meningiomas. If a new treatment modality for meningioma is to be of clinical value, it must be therapeutically effective against malignant meningioma and skull base meningioma involving and infiltrating cranial nerves.

To test the effectiveness of a new treatment modality in skull base meningioma, a patient-like orthotropic model of unresectable meningioma is needed. Several studies have reported xenograft tumor models of skull base meningioma, and IOMM-Lee is the most commonly used cell line. In conventional xenograft meningioma models, tumor cells are implanted using a stereotactic head frame and a bur hole drilled in the frontal bone.[40–44] We implanted IOMM-Lee cells into the lateral part of the foramen ovale in NOG mice to establish meningioma involving the trigeminal nerve. Trigeminal nerve is suitable for histopathologic analysis because it is the largest cranial nerve in rodents. In addition, the integrity of the trigeminal nerve can be

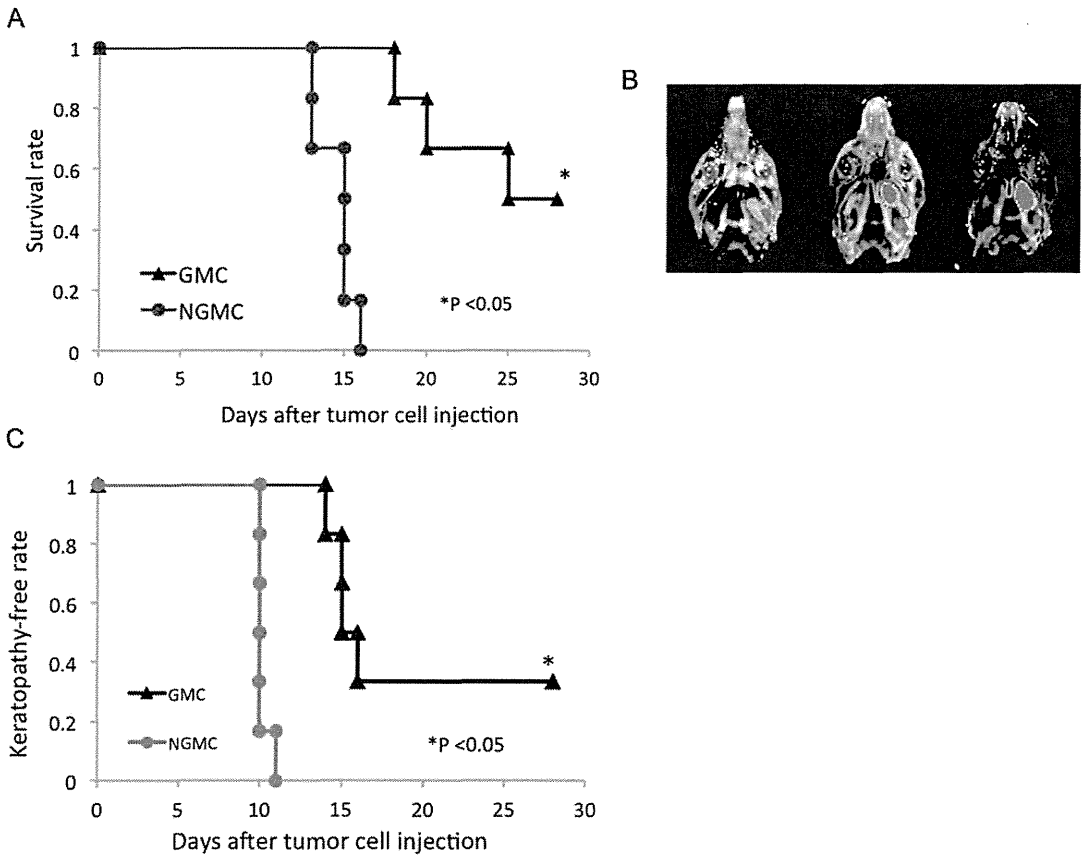


Fig. 5. (A) Survival analysis of skull base meningioma-bearing mice treated with NGMCs and GMCs. The mice received an intravenous injection of NGMCs or GMCs on day 5 after tumor inoculation. There are no survivors among the NGMC-treated mice but 3 survivors among GMC-treated mice by day 28. (B) Three survivors have a small tumor. (C) Effect of adoptive transfer of GMCs on the incidence and time to onset of neurotrophic keratopathy in skull base meningioma-bearing mice. All NGMC-treated mice exhibited neurotrophic keratopathy throughout the observation period. Two GMC-treated mice survived with no symptoms of keratopathy until the experiment was terminated at day 28 after tumor inoculation. These 2 mice were excluded from the statistical analysis of time to onset.

evaluated using the corneal reflex and neurotrophic keratopathy.[26] The trigeminal nerve lies in the medial part of the temporal fossa and has 3 branches, one of which passes through the foramen ovale; the others are located on the medial side of this foramen (Supplementary Material, Fig. S1C and D). In rodents, the PGF is a natural cavity in the rostral area of the opening of the external acoustic meatus, communicating with the temporal fossa (Supplementary Material, Fig. S1C). Thus, the lateral part of the foramen ovale can be easily accessed using the PGFi technique (Supplementary Material, Fig. S1D).[24] The PGFi has technical and anatomical advantages over the conventional implantation technique. The operation time for PGFi is short, requiring ~1 min. In this study, there were no operation-related complications, and skull base meningiomas involving trigeminal nerves were established in all mice. Of intrigue, IOMM-Lee cells infiltrated trigeminal nerve fibers, mimicking the human meningioma infiltration into cranial nerves. Loss of corneal reflex and neurotrophic keratopathy reflected the trigeminal nerve injury caused by tumor infiltration in this mouse model.

In summary, we established a clinically relevant orthotropic model of unresectable meningioma involving the trigeminal nerve that is suitable for preclinical studies. We have shown that WT1 in meningioma cells is a potential target for immunotherapy. WT1-specific T cells recognized and killed meningioma cells in vitro. They retarded the growth of experimental meningioma and the accompanying progression of cranial nerve damage in vivo. Thus, adoptive transfer of WT1-redirected T cells may be an attractive therapeutic approach for difficult-to-treat meningiomas.

## Supplementary Material

Supplementary material is available at *Neuro-Oncology Journal* online (http://neuro-oncology.oxfordjournals.org/).

## Funding

This work was supported by a Grant-in-Aid (B) for Scientific Research from the Japan Society for the Promotion of Science (A.N.).

*Conflict of interest statement.* None declared.

## References


1. Porter DL, Levine BL, Kalos M, Bagg A, June CH. Chimeric antigen receptor-modified T cells in chronic lymphoid leukemia. *N Engl J Med*. 2011;365(8):725–733.
2. Oka Y, Tsuboi A, Oji Y, Kawase I, Sugiyama H. WT1 peptide vaccine for the treatment of cancer. *Curr Opin Immunol*. 2008;20(2):211–220.
3. Ohno S, Kyo S, Myojo S, et al. Wilms' tumor 1 (WT1) peptide immunotherapy for gynecological malignancy. *Anticancer Res*. 2009;29(11): 4779–4784.
4. Okamoto S, Mineno J, Ikeda H, et al. Improved expression and reactivity of transduced tumor-specific TCRs in human lymphocytes by specific silencing of endogenous TCR. *Cancer Res*. 2009;69(23):9003–9011.
5. Ochi T, Fujiwara H, Okamoto S, et al. Novel adoptive T-cell immunotherapy using a WT1-specific TCR vector encoding silencers for endogenous TCRs shows marked antileukemia reactivity and safety. *Blood*. 2011;118(6):1495–1503.
6. Rogers L, Gilbert M, Vogelbaum MA. Intracranial meningiomas of atypical (WHO grade II) histology. *J Neurooncol*. 2010;99(3):393–405.
7. Hanft S, Canoll P, Bruce JN. A review of malignant meningiomas: diagnosis, characteristics, and treatment. *J Neurooncol*. 2010;99(3):433–443.
8. Black P, Kathiresan S, Chung W. Meningioma surgery in the elderly: a case-control study assessing morbidity and mortality. *Acta Neurochir (Wien)*. 1998;140(10):1013–1016; discussion 1016–1017.
9. Black PM, Morokoff AP, Zauberman J. Surgery for extra-axial tumors of the cerebral convexity and midline. *Neurosurgery*. 2008;62(6 suppl 3): 1115–1121; discussion 1121–1113.
10. Sanai N, Sughrue ME, Shangari G, Chung K, Berger MS, McDermott MW. Risk profile associated with convexity meningioma resection in the modern neurosurgical era. *J Neurosurg*. 2010;112(5):913–919.
11. Monleón D, Morales JM, Gonzalez-Segura A, et al. Metabolic aggressiveness in benign meningiomas with chromosomal instabilities. *Cancer Res*. 2010;70(21):8426–8434.
12. Harris AE, Lee JY, Omalu B, Flickinger JC, Kondziolka D, Lunsford LD. The effect of radiosurgery during management of aggressive meningiomas. *Surg Neurol*. 2003;60(4):298–305; discussion 305.
13. Huffmann BC, Reinacher PC, Gilsbach JM. Gamma knife surgery for atypical meningiomas. *J Neurosurg*. 2005;102(suppl):283–286.
14. Stafford SL, Pollock BE, Foote RL, et al. Meningioma radiosurgery: tumor control, outcomes, and complications among 190 consecutive patients. *Neurosurgery*. 2001;49(5):1029–1037; discussion 1037–1028.
15. Larson JJ, van Loveren HR, Balko MG, Tew JM. Evidence of meningioma infiltration into cranial nerves: clinical implications for cavernous sinus meningiomas. *J Neurosurg*. 1995;83(4):596–599.
16. Ohminami H, Yasukawa M, Fujita S. HLA class I-restricted lysis of leukemia cells by a CD8(+) cytotoxic T-lymphocyte clone specific for WT1 peptide. *Blood*. 2000;95(1):286–293.
17. Makita M, Hiraki A, Azuma T, et al. Antilung cancer effect of WT1-specific cytotoxic T lymphocytes. *Clin Cancer Res*. 2002;8(8): 2626–2631.
18. Tsuji T, Yasukawa M, Matsuzaki J, et al. Generation of tumor-specific, HLA class I-restricted human Th1 and Tc1 cells by cell engineering with tumor peptide-specific T-cell receptor genes. *Blood*. 2005; 106(2):470–476.
19. Lee WH. Characterization of a newly established malignant meningioma cell line of the human brain: IOMM-Lee. *Neurosurgery*. 1990; 27(3):389–395; discussion 396.
20. Tanaka K, Sato C, Maeda Y, et al. Establishment of a human malignant meningioma cell line with amplified c-myc oncogene. *Cancer*. 1989;64(11):2243–2249.
21. Ishiwata I, Ishiwata C, Ishiwata E, et al. In vitro culture of various typed meningiomas and characterization of a human malignant meningioma cell line (HKBMM). *Hum Cell*. 2004;17(4):211–217.
22. Neri S, Mariani E, Meneghetti A, Cattini L, Facchini A. Calcein-acetyoxymethyl cytotoxicity assay: standardization of a method allowing additional analyses on recovered effector cells and supernatants. *Clin Diagn Lab Immunol*. 2001;8(6):1131–1135.
23. Ito M, Hiramatsu H, Kobayashi K, et al. NOD/SCID/gamma(c)(null) mouse: an excellent recipient mouse model for engraftment of human cells. *Blood*. 2002;100(9):3175–3182.
24. Iwami K, Momota H, Natsume A, Kinjo S, Nagatani T, Wakabayashi T. A novel method of intracranial injection via the postglenoid foramen for brain tumor mouse models. *J Neurosurg*. 2012;116(3):630–635.
25. Werner SR, Dotzlaf JE, Smith RC. MMP-28 as a regulator of myelination. *BMC Neurosci*. 2008;9:83.
26. Ferrari G, Chauhan SK, Ueno H, et al. A novel mouse model for neurotrophic keratopathy: trigeminal nerve stereotactic electrolysis through the brain. *Invest Ophthalmol Vis Sci*. 2011;52(5):2532–2539.
27. Hutchings Y, Osada T, Woo CY, Clay TM, Lyerly HK, Morse MA. Immunotherapeutic targeting of Wilms' tumor protein. *Curr Opin Mol Ther*. 2007;9(1):62–69.
28. Sugiyama H. Cancer immunotherapy targeting Wilms' tumor gene WT1 product. *Expert Rev Vaccines*. 2005;4(4):503–512.
29. Cheever MA, Allison JP, Ferris AS, et al. The prioritization of cancer antigens: a national cancer institute pilot project for the acceleration of translational research. *Clin Cancer Res*. 2009;15(17):5323–5337.
30. Viola A, Lanzavecchia A. T cell activation determined by T cell receptor number and tunable thresholds. *Science*. 1996;273(5271):104–106.
31. Debets R, Willemsen R, Bolhuis R. Adoptive transfer of T-cell immunity: gene transfer with MHC-restricted receptors. *Trends Immunol*. 2002;23(9):435–436; author reply 436–437.
32. Jorritsma A, Gomez-Eerland R, Dokter M, et al. Selecting highly affine and well-expressed TCRs for gene therapy of melanoma. *Blood*. 2007;110(10):3564–3572.
33. Stauss HJ, Cesco-Gaspere M, Thomas S, et al. Monoclonal T-cell receptors: new reagents for cancer therapy. *Mol Ther*. 2007;15(10): 1744–1750.
34. Cohen CJ, Zhao Y, Zheng Z, Rosenberg SA, Morgan RA. Enhanced antitumor activity of murine-human hybrid T-cell receptor (TCR) in human lymphocytes is associated with improved pairing and TCR/CD3 stability. *Cancer Res*. 2006;66(17):8878–8886.
35. Cohen CJ, Li YF, El-Gamil M, Robbins PF, Rosenberg SA, Morgan RA. Enhanced antitumor activity of T cells engineered to express T-cell receptors with a second disulfide bond. *Cancer Res*. 2007;67(8):3898–3903.
36. Thomas S, Xue SA, Cesco-Gaspere M, et al. Targeting the Wilms tumor antigen 1 by TCR gene transfer: TCR variants improve tetramer binding but not the function of gene modified human T cells. *J Immunol*. 2007;179(9):5803–5810.
37. Heemskerk MH, Hagedoorn RS, van der Hoorn MA, et al. Efficiency of T-cell receptor expression in dual-specific T cells is controlled by the intrinsic qualities of the TCR chains within the TCR-CD3 complex. *Blood*. 2007;109(1):235–243.
38. Kustikova OS, Wahlers A, Kuhlcke K, et al. Dose finding with retroviral vectors: correlation of retroviral vector copy numbers in single cells with gene transfer efficiency in a cell population. *Blood*. 2003;102(12): 3934–3937.
39. Sadelain M. Insertional oncogenesis in gene therapy: how much of a risk? *Gene Ther*. 2004;11(7):569–573.

40. Ragel BT, Couldwell WT, Gillespie DL, Wendland MM, Whang K, Jensen RL. A comparison of the cell lines used in meningioma research. *Surg Neurol*. 2008;70(3):295–307; discussion 307.
41. Ragel BT, Elam IL, Gillespie DL, et al. A novel model of intracranial meningioma in mice using luciferase-expressing meningioma cells. Laboratory investigation. *J Neurosurg*. 2008;108(2):304–310.
42. McCutcheon IE, Friend KE, Gerdes TM, Zhang BM, Wildrick DM, Fuller GN. Intracranial injection of human meningioma cells in athymic mice: an orthotopic model for meningioma growth. *J Neurosurg*. 2000;92(2):306–314.
43. Baia GS, Dinca EB, Ozawa T, et al. An orthotopic skull base model of malignant meningioma. *Brain Pathol*. 2008;18(2):172–179.
44. Salhia B, Rutka JT, Lingwood C, Nutikka A, Van Furth WR. The treatment of malignant meningioma with verotoxin. *Neoplasia*. 2002;4(4):304–311.

Kageyama et al. Journal of Translational Medicine 2013, 11:246
http://www.translational-medicine.com/content/11/1/246

JOURNAL OF TRANSLATIONAL MEDICINE

RESEARCH Open Access

# Dose-dependent effects of NY-ESO-1 protein vaccine complexed with cholesteryl pullulan (CHP-NY-ESO-1) on immune responses and survival benefits of esophageal cancer patients

Shinichi Kageyama[1*†], Hisashi Wada[2†], Kei Muro[3], Yasumasa Niwa[4], Shugo Ueda[5], Hiroshi Miyata[2], Shuji Takiguchi[2], Sahoko H Sugino[1], Yoshihiro Miyahara[1], Hiroaki Ikeda[1], Naoko Imai[1], Eiichi Sato[6], Tomomi Yamada[7], Masaharu Osako[8], Mami Ohnishi[9], Naozumi Harada[9], Tadashi Hishida[9], Yuichiro Doki[2] and Hiroshi Shiku[1]

## Abstract

**Background:** Cholesteryl pullulan (CHP) is a novel antigen delivery system for cancer vaccines. This study evaluated the safety, immune responses and clinical outcomes of patients who received the CHP-NY-ESO-1 complex vaccine, Drug code: IMF-001.

**Methods:** Patients with advanced/metastatic esophageal cancer were enrolled and subcutaneously vaccinated with either 100 μg or 200 μg of NY-ESO-1 protein complexed with CHP. The primary endpoints were safety and humoral immune responses, and the secondary endpoint was clinical efficacy.

**Results:** A total of 25 patients were enrolled. Thirteen and twelve patients were repeatedly vaccinated with 100 μg or 200 μg of CHP-NY-ESO-1 with a median of 8 or 9.5 doses, respectively. No serious adverse events related to the vaccine were observed. Three out of 13 patients in the 100-μg cohort and 7 out of 12 patients in the 200-μg cohort were positive for anti-NY-ESO-1 antibodies at baseline. In the 100-μg cohort, an antibody response was observed in 5 out of 10 pre-antibody-negatives patients, and the antibody levels were augmented in 2 pre-antibody-positive patients after vaccination. In the 200-μg cohort, all 5 pre-antibody-negative patients became seropositive, and the antibody level was amplified in all 7 pre-antibody-positive patients. No tumor shrinkage was observed. The patients who received 200 μg of CHP-NY-ESO-1 survived longer than patients receiving 100 μg of CHP-NY-ESO-1, even those who exhibited unresponsiveness to previous therapies or had higher tumor burdens.

**Conclusions:** The safety and immunogenicity of CHP-NY-ESO-1 vaccine were confirmed. The 200 μg dose more efficiently induced immune responses and suggested better survival benefits. (Clinical trial registration number NCT01003808).

**Keywords:** Esophageal cancer, Cancer vaccine, NY-ESO-1, Cholesteryl pullulan (CHP)

* Correspondence: kageyama@clin.medic.mie-u.ac.jp
†Equal contributors
[1]Departments of Immuno-Gene Therapy and Cancer Vaccine, Mie University Graduate School of Medicine, 2-174, Edobashi, Tsu, Mie 514-8507, Japan
Full list of author information is available at the end of the article

## Background

Complexes of cholesteryl pullulan (CHP) nano-particles that contain a tumor antigen are a new type of cancer vaccine with a novel antigen delivery system that presents multiple epitope peptides to both the MHC class I and class II pathways [1-4]. We have been developing CHP-protein human cancer vaccines that efficiently induce immune responses against multiple T cell epitopes for various HLA types. Previous clinical studies using CHP-HER2 and CHP-NY-ESO-1 vaccines showed that these vaccines could be administered repeatedly without serious adverse effects, and both vaccines induced antigen-specific $CD4^+$ and $CD8^+$ T cell immunity as well as humoral immunity [5-7].

Because the NY-ESO-1 antigen is a cancer-testis antigen that is exclusively expressed in the tumor tissue, aside from expression in the normal testis and placenta, this antigen is considered an ideal target for cancer immunotherapy [8,9].

The appropriate dose for NY-ESO-1 protein vaccine has not been determined, although doses up to 100 μg have been examined, in which a higher dose was more immunogenic compared to lower doses of 10 μg and 30 μg [10].

We conducted a dose-escalating trial with CHP-NY-ESO-1 vaccine doses of 100 μg and 200 μg for esophageal cancer patients who were resistant to standard therapies. We evaluated the safety and immune responses to the NY-ESO-1 antigen over the vaccination period, and explored the clinical impact on esophageal cancer patients with a poor prognosis.

In this study, we analyzed IgG antibody responses as antigen-specific immune responses. Although T cells that are induced by a cancer vaccine should be evaluated as an immune-monitoring marker, T cells can be difficult to detect directly and quantitatively assess, whereas IgG titers measured by ELISA could act as a suitable immune-monitoring marker. Analyzing antibody responses induced by CHP-NY-ESO-1 vaccine, the 200 μg-dose more efficiently induced immune responses and suggested better survival benefits.

## Materials and methods

### Preparation of CHP-NY-ESO-1 complex vaccine

CHP-NY-ESO-1 complex vaccine (Drug code: IMF-001) was provided by ImmunoFrontier, Inc. (Tokyo, Japan). All processes were performed following current Good Manufacturing Practices (cGMP) conditions. The toxicity of the drug products was assessed using animal models, and stability was monitored during the clinical trial using representative samples of the investigational drug product.

### Study design

This study was a phase 1, open-label, multi-institutional, dose-escalating clinical trial of the CHP-NY-ESO-1 complex vaccine administered subcutaneously to patients with unresectable, advanced, or refractory esophageal tumors that expressed the NY-ESO-1 antigen. The primary objective was to determine the maximum tolerated dose (MTD) and the biological recommended dose, and the secondary objective was to assess clinical efficacy.

Patients were eligible for entry, if they had a performance status of 0, 1, or 2, were at least 20 years old, had a life expectancy of 4 months or more, and did not have impaired organ function. Patients were ineligible if they were positive for HIV antibody, had multiple cancers, autoimmune disease, serious allergy history, or active brain metastasis, or received previous chemotherapy, systemic steroid or immunosuppressive therapy within less than 4 weeks.

The patients were divided into the following two cohorts of 10 patients each: Cohort 1, 100 μg of the NY-ESO-1 protein every two weeks, and Cohort 2, 200 μg of the NY-ESO-1 protein every two weeks. When a patient withdrew from the trial within three vaccinations, they were replaced with an additional patient.

Clinical responses were assessed according to the Response Evaluation Criteria in Solid Tumors (RECIST ver1.1) [11] and its modified version. The modified version is based on immune-related Response Criteria (ir-RC) [12] and includes the following: Tumor responses were assessed every 6 weeks. Even if disease progression was observed within the first 12 weeks, PD (progressive disease) was not judged. When disease progression was observed after 18 weeks, PD was determined.

Each patient received 6 administrations. However, the treatment could be continued beyond this period if the patient wished to maintain treatment and met the following criteria: 1) no evidence of tumor progression or worsening of performance status (PS), and 2) an anti-NY-ESO-1 antibody response was confirmed. Safety was evaluated according to the National Cancer Institute Common Terminology Criteria for Adverse Events ver.3.0 (NCI-CTCAE ver.3.0) [13]. All the safety information was collected and evaluated, and dose escalation was judged by the Independent Data and Safety Committee.

The study was performed in accordance with the current version of the Declaration of Helsinki and Good Clinical Practice. Written informed consent was obtained from all patients participating in this study. The protocol was approved by the institutional review board at each site. The clinical trial was sponsored by ImmunoFrontier, Inc. (Tokyo, Japan), and registered as ID: NCT01003808 of ClinicalTrials.Gov.

### Expression of NY-ESO-1 antigen

NY-ESO-1 expression was assessed by immunohistochemistry with the monoclonal antibody, E978 (Sigma-Aldrich, Saint Louis, MO), [9] or quantitative RealTime-PCR (qRT-PCR) using specific primers [14].

### Serum samples

To analyze antigen-specific antibody responses, sera were collected at baseline and two weeks after each vaccination. All sera were stored at −80°C until analysis.

### Antibody responses to NY-ESO-1 antigen

NY-ESO-1-specific antibodies in the sera were measured by ELISA as described previously [15]. Briefly, recombinant NY-ESO-1 proteins (His-tag and GST-tag) and NY-ESO-1 peptides were absorbed onto immunoplates (442404; Nunc, Roskilde, Denmark) at a concentration of 10 ng/50 μL/well at 4°C. The collected serum samples were diluted from 1:400 to 1:102,400. After washing and blocking the plate, the sera were added and incubated for 10 h. After washing, goat anti-human IgG (H + L chain) (MBL, Nagoya, Japan) conjugated with peroxidase (The Binding Site, San Diego, CA) was added. After adding the TMB substrate (Pierce, Rockford, IL), the plate was read using a Microplate Reader (model 550; Bio-Rad, Hercules, CA).

Serum samples for 80 healthy volunteers were evaluated to determine a cut-off level for the anti-NY-ESO-1 antibody based on the optical density $(OD)_{450-550}$ absorption value. The cut-off level of anti-NY-ESO-1 IgG was 0.182. A sample was considered to be positive for anti-NY-ESO-1 antibodies if the optical density $(OD)_{450-550}$ absorption value in the ELISA was at the cut-off level or higher at a serum dilution of 1:400. The immune responses of patients with pre-existing anti-NY-ESO-1 antibodies were judged as augmentation if the serum diluted 4-fold or more remained positive.

### Statistical analysis

Rates of the immune responses between the patients in Cohort 1 and Cohort 2 were compared by Fisher's exact test, and the survival curve was estimated using the Kaplan–Meier method and compared by the log-rank test. In order to adjust the confounding factors, Cox proportional hazards model was applied. All analyses were done using SAS 9.2 (SAS Institute Inc., Cary, NC).

## Results and discussion

### Patient characteristics and clinical safety

A total of 25 patients were enrolled in the clinical trial. All patients had unresectable, advanced, or refractory esophageal cancers. The tumor cells in all of these patients were NY-ESO-1-positive, in which the positivity was determined by immunohistochemistry and qRT-PCR for 24 patients and one patient, respectively. All patients received standard chemotherapy and/or other cancer therapies including radiotherapy and surgery, which were ultimately ineffective (Table 1).

Cohort 1 consisted of 13 patients who were given 100 μg of the vaccine; Cohort 2 consisted of 12 patients who were given 200 μg of the vaccine. The patients in Cohort 1 and Cohort 2 received 2 to 27 vaccinations with a median of 8 doses and 3 to 21 vaccinations with a median of 9.5 doses, respectively (Table 1). No dose-limiting toxicity (DLT) was observed. All the patients except one developed transient, grade 1 skin reactions at the injection sites. Other adverse events included swallowing disturbance (n = 8), diarrhea (n = 3), and fever (n = 2), in which events of grade 3 or 4 were included. These events were considered unrelated to the CHP-NY-ESO-1 vaccination. Based on the laboratory data, decreased lymphocyte counts were observed (n = 10), which were all grade 3. These patients had lymphopenia at baseline, probably due to the previous chemotherapies. During the course of the vaccinations, they developed grade 3 lymphopenia, which were shifted from the other grade of the pre-vaccine lymphopenia. Other changes included decreased Na levels (n = 4), decreased hemoglobin levels (n = 3), elevated transaminase levels (n = 2) and elevated uric acid (n = 2) (Table 2). These adverse events were changed from the decreased or elevated levels at baseline. They did not affect the vaccine continuation. Therefore, the changes were considered not related or unlikely related to the vaccination.

**Table 1 Patients demographics**

| | 100 μg | 200 μg |
|---|---|---|
| No. patients enrolled | 13 | 12 |
| Sex | | |
| Male | 13 | 11 |
| Female | 0 | 1 |
| Age | | |
| Median | 69 | 64.5 |
| Range | 49-72 | 53-79 |
| Prior therapy | | |
| Surgery | 6 | 5 |
| Radiotherapy | 11 | 7 |
| Chemotherapy | 13 | 12 |
| Pre-existing antibody to NY-ESO-1 antigen | 3 | 7 |
| No. vaccinations | | |
| Median | 8 | 9.5 |
| Range | 2-27 | 3-21 |

### Immune responses to NY-ESO-1 protein

As shown Table 3, 3 out of the 13 patients, and 7 out of 12 patients had pre-existing antibodies to NY-ESO-1, while the remaining 10 and 5 patients did not have this reactivity in Cohort 1 and Cohort 2, respectively.

To evaluate the antibody responses after vaccination, serum samples collected at the serial vaccinations were analyzed using an antigen-specific IgG ELISA. In three patients of 100–02, 100–3 and 200–7 who were vaccinated three times, the serum samples from 1st and 2nd

**Table 2 Adverse events during CHP-NY-ESO-1 vaccinations**

| Adverse event | 100 μg(n = 13) | | | | | | 200 μg(n = 12) | | | | | | Total |
|---|---|---|---|---|---|---|---|---|---|---|---|---|---|
| | Grade | | | | | | Grade | | | | | | |
| | 1 | 2 | 3 | 4 | 5 | Subtotal | 1 | 2 | 3 | 4 | 5 | Subtotal | |
| Skin reaction | 12 | 0 | 0 | 0 | 0 | 12 | 12 | 0 | 0 | 0 | 0 | 12 | 24 |
| Swallowing disturbance | 0 | 0 | 3 | 0 | 0 | 3 | 0 | 0 | 4 | 1 | 0 | 5 | 8 |
| Diarrhea | 0 | 0 | 2 | 0 | 0 | 2 | 1 | 0 | 0 | 0 | 0 | 1 | 3 |
| Fever | 2 | 0 | 0 | 0 | 0 | 2 | 0 | 0 | 0 | 0 | 0 | 0 | 2 |
| Decreased lymphocytes count | 0 | 0 | 7 | 0 | 0 | 7 | 0 | 0 | 3 | 0 | 0 | 3 | 10 |
| Decreased Na level | 0 | 0 | 2 | 0 | 0 | 2 | 0 | 0 | 2 | 0 | 0 | 2 | 4 |
| Decreased Hb level | 0 | 0 | 3 | 0 | 0 | 3 | 0 | 0 | 0 | 0 | 0 | 0 | 3 |
| Elevated ALT/AST level | 0 | 0 | 2 | 0 | 0 | 2 | 0 | 0 | 0 | 0 | 0 | 0 | 2 |
| Elevated uric acid level | 0 | 0 | 1 | 1 | 0 | 2 | 0 | 0 | 0 | 0 | 0 | 0 | 2 |

NOTE: Events occurring more than once are listed. Events of disease progression are not listed.

vaccination were assayed. In Cohort 1, out of 10 pre-antibody-negative patients, 5 became seropositive. Two out of 3 pre-antibody-positive patients had augmented antibody responses. In total, 7 of 13 (53.8%) patients exhibited immune responses. Five pre-antibody-negative and 7 pre-antibody-positive patients in Cohort 2 became positive or were augmented, yielding 12 out of 12 or 100% responsiveness. The 200-μg dose was more immunogenic than the 100-μg dose ($p = 0.015$, Fisher's exact test). In Cohort 1, immune reactions were observed after a median of 2 cycles, with a range of 1 to 4 vaccine cycles. In Cohort 2, the immune responses were also evident after a median of 2 cycles with a range of 1 to 5 cycles (Table 3). The chronological appearance of the immune responses and antibody titers are shown in Figure 1. The antibody intensities appeared more quickly and at a higher titer in patients in Cohort 2 (200 μg) than those in Cohort 1(100 μg). In addition to His-tag NY-ESO-1 protein, we tested serum reactivities to GST-tag NY-ESO-1 protein and NY-ESO-1 peptides. We confirmed specific reactions to NY-ESO-1 antigen in these sera.

### Clinical responses and long-term follow-up

There were no cases of tumor shrinkage with partial response (PR) or complete response (CR) in any of the 25 patients. At the assessment that occurred every 6 weeks after vaccination, stable disease (SD) was observed in 3 patients in Cohort 1 and 6 patients in Cohort 2 (Table 4). There was no discordance in the evaluations between RECIST ver1.1 [11] and its modified version [12].

**Table 3 Antibody responses in patients vaccinated with 100 μg or 200 μg of CHP-NY-ESO-1**

| 100 μg | | | | 200 μg | | | |
|---|---|---|---|---|---|---|---|
| pt No. | Vaccination cycle | Baseline (dilution titer) | Antibody response (cycle*) | pt No. | Vaccination cycle | Baseline (dilution titer) | Antibody response (cycle*) |
| 100-01 | 9 | negative | responded(4) | 200-01 | 15 | negative | responded(2) |
| 100-02 | 3 | negative | no response** | 200-02 | 9 | negative | responded(2) |
| 100-03 | 3 | negative | no response** | 200-03 | 8 | positive (x1,600) | responded(5) |
| 100-04 | 7 | negative | no response | 200-04 | 21 | negative | responded(2) |
| 100-05 | 2 | negative | no response | 200-05 | 3 | negative | responded(2) |
| 100-06 | 16 | positive (x6,400) | responded(1) | 200-06 | 10 | positive (x400) | responded(1) |
| 100-07 | 9 | positive (x25,600) | no response | 200-07 | 3 | positive (x25,600) | responded(2)** |
| 100-08 | 10 | negative | responded(1) | 200-08 | 11 | positive (x400) | responded(1) |
| 100-09 | 5 | negative | no response | 200-09 | 18 | positive (x400) | responded(3) |
| 100-10 | 27 | positive (x400) | responded(3) | 200-10 | 11 | positive (x400) | responded(2) |
| 100-11 | 8 | negative | responded(2) | 200-11 | 3 | positive (x400) | responded(2) |
| 100-12 | 8 | negative | responded(2) | 200-12 | 9 | negative | responded(1) |
| 100-13 | 26 | negative | responded(2) | | | | |
| antibody response rate | | | 53.8%*** | | | 100%*** | |

*vaccine cycles with which antibody responses appeared. **antibody responses assayed after two vaccinations.***p = 0.015(Fisher's exact test).

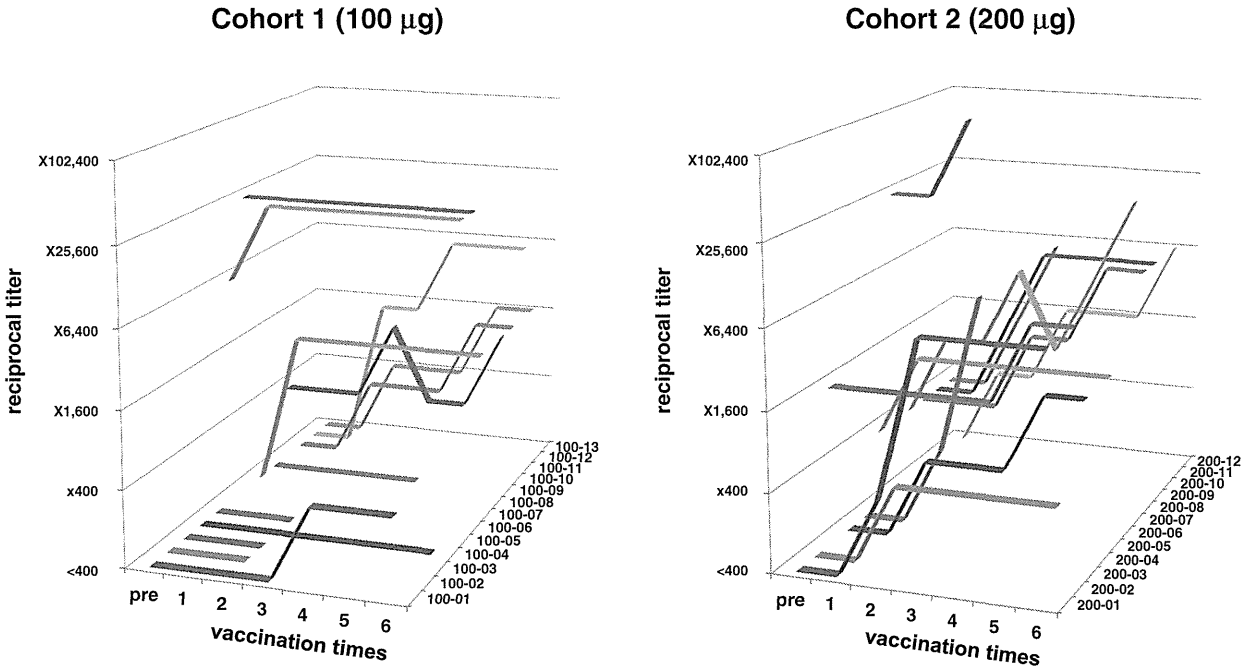


**Figure 1 Antibody responses to recombinant NY-ESO-1 protein as determined by ELISA.** Sera from 13 patients in Cohort 1 (100-μg dose) and 12 patients in Cohort 2 (200-μg dose) were collected at each vaccination, and serially diluted by 400, 1,600, 6,400, 25,600 and 102,400. Reciprocal titers were determined based on the maximally diluted sera, which showed a higher OD (optical density of 450–500) value than the cut-off level for NY-ESO-1 antibody positivity.

The disease progression-free survival time was 11 weeks on average, with a median of 6 weeks and range of 4 to 52 weeks. In Cohort 1 (n = 13), patients who were vaccinated with 100 μg of CHP-NY-ESO-1 survived without disease progression for 11 weeks on average, with a median of 6 weeks and range of 4 to 52 weeks. In Cohort 2 (n = 12) in which patients received the 200-μg dose, the patients were progression-free for 10 weeks on average, with a median of 8.5 weeks and range of 6 to 18 weeks (Table 4). There was no difference between the two cohorts (p = 0.748, Figure 2-A).

The overall survival time was 33 weeks on average, with a median of 31 weeks and range of 4 to 72 weeks. In Cohort 1 (n = 13), the patients survived for 25 weeks on average, with a median of 23 weeks and range of 4 to 60 weeks. In Cohort 2 (n = 12), they survived for 41 weeks on average, with a median of 41 weeks and range of 8 to 72 weeks (Table 4). The patients vaccinated with 200 μg of CHP-NY-ESO-1 had statistically longer survival than those who received the 100-μg dose (p = 0.050, Figure 2-B). Each cohort included three patients who were vaccinated three times or less because of early disease progression, and were withdrawn from this study, respectively. Having excluded those 6 patients, the patients vaccinated with 200 μg-vaccine still had longer survival than those with 100 μg-vaccinations (data not shown).

When the survival of patients who had responded to previous therapies (n = 12) was compared to non-responders (n = 13), the responders lived longer than the non-responders after vaccination (p = 0.005, Figure 2-C). The patients who never responded to previous therapies and received the 200-μg dose (n = 6) significantly lived longer than those who received the 100-μg dose (n = 7) (p = 0.029, Figure 2-D).

When the survival of patients who had tumors with a maximal diameter of 30 mm or less, including non-measurable lesions (n = 13) was compared with those with diameters more than 30 mm (n = 12), the patients with higher tumor burdens had shorter life spans (p = 0.021, Figure 2-E). Among patients with higher tumor burdens, patients who were vaccinated with the 200-μg dose (n = 4) lived longer than those who received the 100-μg dose (n = 8), (p = 0.037, Figure 2-F).

Using Cox proportional hazards models, the vaccine dose and the responsiveness to previous therapy were independent factors that influenced the overall survival, which showed p = 0.011 with HR 3.595 (95%CI 1.335-9.678) and p = 0.002 with HR 0.194 (95%CI 0.068-0.553), respectively. Also, the vaccine dose and the tumors sizes including non-measurable disease independently affected the overall survival, showing p = 0.040 with HR 2.630 (95%CI 1.045-6.614) and p = 0.020 with HR 0.322 (95%CI 0.124-0.833), respectively.

**Table 4 Baseline clinical profiles and responses after CHP-NY-ESO-1 vaccinations**

| 100 μg | | | | | | 200 μg | | | | | |
|---|---|---|---|---|---|---|---|---|---|---|---|
| pt No. | Response to previous therapies (duration time, weeks) | *sum of tumor diameters (mm) | Tumor response (BOR) | Time-to-progression (weeks) | Survival (weeks) | pt No. | Response to previous therapies (duration time, weeks) | *sum of tumor diameters (mm) | Tumor response (BOR) | Time-to-progression (weeks) | Survival (weeks) |
| 100-01 | PR (4) | NA | PD | 6 | 31 | 200-01 | PR (29) | 24 | SD | 17 | 70 |
| 100-02 | SD | 53 | NE | 4 | 6 | 200-02 | NE | 25 | SD | 18 | 33 |
| 100-03 | NE | 144 | NE | 4 | 6 | 200-03 | PR (32) | 55 | PD | 6 | 37 |
| 100-04 | PD | 182 | PD | 5 | 17 | 200-04 | PR (30) | NA | PD | 6 | 50 |
| 100-05 | CR (38) | 101 | NE | 4 | 4 | 200-05 | PR (32) | NA | PD | 6 | 72 |
| 100-06 | SD | 69 | PD | 6 | 31 | 200-06 | NE | 32 | SD | 18 | 54 |
| 100-07 | CR (15) | 78 | PD | 6 | 29 | 200-07 | NE | 205 | NE | 6 | 8 |
| 100-08 | NE | 39 | SD | 18 | 23 | 200-08 | PR (12) | 16 | SD | 11 | 33 |
| 100-09 | SD | 18 | PD | 6 | 8 | 200-09 | CR (96) | 88 | PD | 6 | 45 |
| 100-10 | CR (24) | NA | SD | 11 | 60 | 200-10 | SD | NA | SD | 12 | 48 |
| 100-11 | SD | 31 | SD | 12 | 20 | 200-11 | SD | NA | NE | 6 | 12 |
| 100-12 | PR (9) | NA | NE | 16 | 28 | 200-12 | SD | NA | SD | 12 | 33 |
| 100-13 | PR (16) | NA | NE | 52 | 59 | | | | | | |

*target lesions determined based on RECIST criteria.

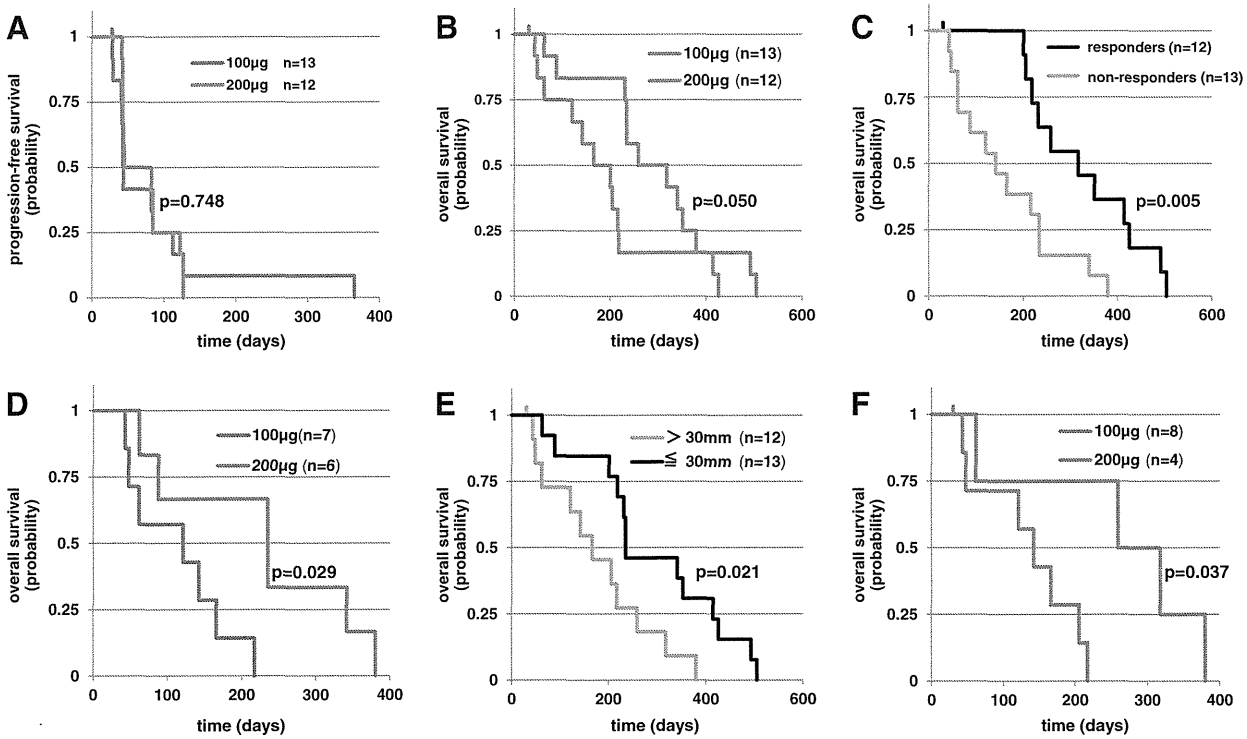


**Figure 2 Kaplan-Meier survival curves of patients who were alive after the CHP-NY-ESO-1 vaccinations. A**: Progression-free survival (PFS) of patients assigned to Cohort 1 (100-μg dose, n = 13) or Cohort 2 (200-μg dose, n = 12). The probability of PFS of the patients who received 200 μg of the vaccine and those who received the 100-μg dose were similar (log-rank test, p = 0.748). **B**: Overall survival (OS) of patients assigned to Cohort 1 or Cohort 2. The patients who received 200 μg of the vaccine survived longer than those who received the 100-μg dose. (log-rank test, p = 0.050). **C**: OS of patients vaccinated with either 100 μg or 200 μg of CHP-NY-ESO-1 compared between patients who responded to previous therapies and those who never responded. The patients who responded to previous therapies and were vaccinated with CHP-NY-ESO-1 survived longer than non-responders. (log-rank test, p = 0.0050). **D**: OS of patients vaccinated with 100 μg or 200 μg of CHP-NY-ESO-1 who never responded to previous therapies. The patients who received 200 μg of the vaccine survived longer than those who received the 100-μg dose (log-rank test, p = 0.029). **E**: OS of patients vaccinated with 100 μg or 200 μg of CHP-NY-ESO-1 compared with either baseline tumor burdens of >30 mm (sum of the tumor diameters) or 30 mm or less including non-measurable lesions. The patients with a tumor burden higher than 30 mm had reduced survival compared to those with smaller burdens (log-rank test, p = 0.021). **F**: OS of patients who received 100 μg or 200 μg of CHP-NY-ESO-1 who had baseline tumor burdens greater than 30 mm. The patients who received 200 μg of the vaccine survived longer than those who received the 100-μg dose (log-rank test, p = 0.037).

This study was a phase 1 dose-escalating clinical trial that examined two doses of the CHP-NY-ESO-1 vaccine in esophageal cancer patients. The primary goals were to evaluate the vaccine safety and immune responses to the NY-ESO-1 antigen, and we further explored the clinical effects on esophageal cancer patients with a poor prognosis.

CHP consists of a hydrophobic polysaccharide pullulan containing chemically introduced cholesterol groups, which spontaneously aggregate to form nano-sized particles that can contain antigen proteins. Using this system as a vaccine, tumor antigen proteins delivered to antigen-presenting cells can stimulate both antigen-specific CD4+ T cells and CD8+ T cells. In a pre-clinical study, dendritic cells pulsed with the CHP-NY-ESO-1 complex could induce both NY-ESO-1-specific CD4+ and CD8+ T cells [4]. Previous clinical studies using CHP-HER2 and CHP-NY-ESO-1 vaccines have shown that these vaccines can induce antigen-specific $CD4^+$ and $CD8^+$ T cell immunity in cancer patients [5-7].

In the current study, we found that CHP-NY-ESO-1 was clinically safe and that the immune responses to the NY-ESO-1 antigen, which were evaluated based on IgG antibody titers, showed a dose-dependent effect between the 100-μg dose and 200-μg. Furthermore, the survival rates of patients who were vaccinated with the 200-μg dose were superior to those who received the 100-μg dose. The patients had recurrent or metastatic esophageal tumors that exhibited clinical resistance to chemotherapy or radiotherapy. The first 13 patients were enrolled to Cohort 1, and the next 12 patients were included in Cohort 2. As the clinical backgrounds of the two cohorts were similar, it was reasonable to make a comparative consideration.

As the previous NY-ESO-1 protein vaccine trials have demonstrated, the toxicity of the CHP-vaccine was very

mild. Grade 3 swallowing disturbances were seen, which were likely related to the progression of esophageal cancer. The other grade 3 events included diarrhea, which was not related to the vaccine. The only related events were grade 1 skin reactions at the injection sites.

Previous vaccine trials have used recombinant full-length NY-ESO-1 protein with various adjuvants. Melanoma patients were divided into three cohorts that were vaccinated with 10 μg, 30 μg or 100 μg of the NY-ESO-1 protein in combination with the saponin adjuvant ISCOMATRIX [10]. The 100-μg dose of NY-ESO-1 induced more immune responses than the other two doses. The responses were evaluated based on IgG antibody titers and delayed-type hypersensitivity (DTH) of skin reactions. In the CHP system, a single 100-μg dose of CHP-NY-ESO-1 was examined with or without the adjuvant OK-432 [6,7,16]. These reports suggested that the 100-μg dose of CHP-NY-ESO-1 is sufficient to induce immune responses. The current trial was designed to determine whether the NY-ESO-1 protein vaccine has potential dose-dependent effects on immunogenicity in patients with homogeneous backgrounds. By assessing humoral immune responses in the cohorts that received 100 μg and 200 μg of the vaccine, the responses appeared in the early phases. We initially intended to analyze antibodies using samples from patients who were vaccinated for at least 4 cycles, as we thought it could take at least 4 cycles to detect immune responses. In the overall data acquisition, samples from all 25 patients were analyzed, which included sera from at least two vaccinations. In conclusion, we found that the 200-μg dose was more efficient than the 100-μg dose.

The other reports included vaccine studies using recombinant NY-ESO-1 protein in combination with Imiquimod and CpG [17,18]. In these studies, the NY-ESO-1 protein was given at doses of 100 μg, and 100 μg or 400 μg, respectively. Based on the patients' sera, the 400-μg dose might have induced more antibody responses than the 100-μg dose, but this was not statistically analyzed. Combined with these reports, the NY-ESO-1 protein might be immunogenic at increasing doses of 10 μg, 30 μg, 100 μg and 200 μg. Since dose-limited toxicity (DLT) was not observed at the higher dose of 200 μg in this study, additional dose increments might be acceptable to determine whether higher doses can induce stronger immune responses.

In this study, we explored a long-term clinical outcome of the NY-ESO-1 protein vaccine. This study was not initially designed to detect a statistical significance of the clinical effect between the 2 cohorts. Instead, we made a comparison to find out if there might include a positive signal for further clinical trials of this vaccine. The NY-ESO-1 protein vaccine with the adjuvant ISCOMATRIX suggested that melanoma patients who were vaccinated after standard therapy tended to have fewer relapses [10], which were not statistically analyzed. The other studies reported that vaccinations with NY-ESO-1-expressing poxvirus vectors and NY-ESO-1 overlapping peptides both prolonged progression-free survivals in ovarian cancer patients who did not have measurable disease after standard therapy [19,20]. In this study, most of the patients developed disease-progression in 6 months, and there was no difference between the patients vaccinated with 100 μg and 200 μg of the CHP-NY-ESO-1, as the previous studies demonstrated that disease-progression occurs in the early phase of vaccinations [12,21].

In contrast, we found that dose-dependent effects of the CHP-NY-ESO-1 vaccine on overall survival of patients with advanced/metastatic esophageal cancer. Analyzing other clinical categories, both the baseline tumor sizes and the tumor responsiveness to previous therapies were significant factors influencing the overall survival. Using Cox proportional hazards models, it was indicated that the tumor sizes and the vaccine doses independently influenced the survival. In the same way, the responsiveness to previous therapies and the vaccine doses independently affected the survival. Therefore, it is suggested that the higher dose of CHP-NY-ESO-1 vaccine played a role in prolongation of the overall survival in the esophageal cancer patients.

In addition, the higher-dose of the vaccine provided significant survival benefit in patients who never responded to the previous therapies or had larger tumor burdens than the lower dose vaccinations. It is difficult to discuss why the patients with a poorer prognosis were more benefited from the 200-μg dose of the vaccine than 100-μg. It might be speculated that the dose-dependency clinical benefits were more often observable in patients with a poorer prognosis, because they might have needed more immune responses in order to survive longer by preventing disease deterioration.

In the previous CHP-NY-ESO-1 vaccine study, which was a phase 1 study that enrolled various types of NY-ESO-1-expressing cancer patients, tumor regression was observed in two out of four esophageal cancer patients [6]. However, tumor shrinkage is rarely observed in cancer vaccine therapies, although some disease stabilization is seen. This study shows that clinical benefits, such as long-term survival, can be detected if a clinical trial is designed in a comparative way. The results were not compared to unvaccinated controls, and it is not possible to directly determine the effects of the vaccine, but is possible to reasonably interpret the effects of immune response on the clinical outcomes.

## Conclusions

The safety and immunogenicity of the CHP-NY-ESO-1 vaccine were confirmed in the patients with antigen-expressing esophageal cancer. The 200-μg dose efficiently induced antigen-specific immune responses and suggested better survival benefits, even for patients with a poorer prognosis. In future clinical trials, 200 μg will be the recommended dose.

**Abbreviations**
BOR: Best overall response; NA: Not available; NE: Not evaluable.

**Competing interests**
This study is supported by ImmunoFrontier, Inc. and Naozumi Harada is an employee, and Mami Ohnishi and Tadashi Hishida are former employees of ImmunoFrontier, Inc. Hiroshi Shiku is a stockholder of ImmunoFrontier, Inc.

**Authors' contributions**
SK, HW, KM, YN, SU, HM, ST and YD treated patients and provided the clinical data. SHS and YM worked on immune responses. HI, NI and ES evaluated tumor antigen expression. TY, MOs and MOh worked on the study statistics. NH and TH were responsible for manufacturing the study drug. SK and HS wrote the manuscript. All authors read and approved the final manuscript.

**Acknowledgements**
We thank all co-workers from all units of Osaka University Hospital, Mie University Hospital, Kitano Hospital and Aichi Cancer Center Hospital for their skills in making this trial run successfully and for the support they provided to the patients under their care. We also thank all co-workers from FiveRings, Co. Ltd. and Statcom Co. Ltd. for operating and analyzing this study. We express thanks to Mr. Masanobu Kimura, Dr. Keigo Hanada (ImmunoFrontier, Inc.) and Mr. Hiroshi Miyamoto (FiveRings, Co. Ltd.) for their special contributions to operating this clinical trial.

**Author details**
[1]Departments of Immuno-Gene Therapy and Cancer Vaccine, Mie University Graduate School of Medicine, 2-174, Edobashi, Tsu, Mie 514-8507, Japan. [2]Department of Gastroenterological Surgery, Osaka University Graduate School of Medicine, Yamadaoka 2-2 (E2), Suita, Osaka 565-0871, Japan. [3]Department of Clinical Oncology, Aichi Cancer Center Hospital, 1-1Kanokoden, Chikusa-ku Nagoya 464-8681, Japan. [4]Department of Endoscopy, Aichi Cancer Center Hospital, 1-1Kanokoden, Chikusa-ku Nagoya 464-8681, Japan. [5]Department of Gastroenterological Surgery and Oncology, Kitano Hospital, The Tazuke Kofukai Medical Research Institute, 2-4-20 Ohgimachi, Kita-ku, Osaka 530-8480, Japan. [6]Department of Anatomic Pathology, Tokyo Medical University, 6-1-1Shinjuku, Shinjuku-ku, Tokyo 160-8402, Japan. [7]Department of Translational Medical Science, Mie University Graduate School of Medicine, 2-174, Edobashi, Tsu, Mie 514-8507, Japan. [8]FiveRings, Co. Ltd, 9-4, 2-chome, Higashi-Tenman, Kita-ku, Osaka 530-0044, Japan. [9]ImmunoFrontier, Inc, 5-10, 2-chome, Sannou, Ota-ku, Tokyo 143-0023, Japan.

Received: 13 July 2013 Accepted: 30 September 2013
Published: 5 October 2013

**References**

1. Gu XG, Schmitt M, Hiasa A, Nagata Y, Ikeda H, Sasaki Y, Akiyoshi K, Sunamoto J, Nakamura H, Kuribayashi K, Shiku H: **A novel hydrophobized polysaccharide/oncoprotein complex vaccine induces in vitro and in vivo cellular and humoral immune responses against HER2-expressing murine sarcomas.** *Cancer Res* 1998, **58**:3385–3390.
2. Ikuta Y, Katayama N, Wang L, Okugawa T, Takahashi Y, Schmitt M, Gu X, Watanabe M, Akiyoshi K, Nakamura H, Kuribayashi K, Sunamoto J, Shiku H: **Presentation of a major histocompatibility complex class 1-binding peptide by monocyte-derived dendritic cells incorporating hydrophobized polysaccharide-truncated HER2 protein complex: implications for a polyvalent immuno-cell therapy.** *Blood* 2002, **99**:3717–3724.
3. Wang L, Ikeda H, Ikuta Y, Schmitt M, Miyahara Y, Takahashi Y, Gu X, Nagata Y, Sasaki Y, Akiyoshi K, Sunamoto J, Nakamura H, Kuribayashi K, Shiku H: **Bone marrow-derived dendritic cells incorporate and process hydrophobized polysaccharide/oncoprotein complex as antigen presenting cells.** *Int J Oncol* 1999, **14**:695–701.
4. Hasegawa K, Noguchi Y, Koizumi F, Uenaka A, Tanaka M, Shimono M, Nakamura H, Shiku H, Gnjatic S, Murphy R, Hiramatsu Y, Old LJ, Nakayama E: **In vitro stimulation of CD8 and CD4 T cells by dendritic cells loaded with a complex of cholesterol-bearing hydrophobized pullulan and NY-ESO-1 protein: Identification of a new HLA-DR15-binding CD4 T-cell epitope.** *Clin Cancer Res* 2006, **12**:1921–1927.
5. Kitano S, Kageyama S, Nagata Y, Miyahara Y, Hiasa A, Naota H, Okumura S, Imai H, Shiraishi T, Masuya M, Nishikawa M, Sunamoto J, Akiyoshi K, Kanematsu T, Scott AM, Murphy R, Hoffman EW, Old LJ, Shiku H: **HER2-specific T-cell immune responses in patients vaccinated with truncated HER2 protein complexed with nanogels of cholesteryl pullulan.** *Clin Cancer Res* 2006, **12**:7397–7405.
6. Uenaka A, Wada H, Isobe M, Saika T, Tsuji K, Sato E, Sato S, Noguchi Y, Kawabata R, Yasuda T, Doki Y, Kumon H, Iwatsuki K, Shiku H, Monden M, Jungbluth AA, Ritter G, Murphy R, Hoffman E, Old LJ, Nakayama E: **T cell immunomonitoring and tumor responses in patients immunized with a complex of cholesterol-bearing hydrophobized pullulan (CHP) and NY-ESO-1 protein.** *Cancer Immun* 2007, **7**:9–19.
7. Kawabata R, Wada H, Isobe M, Saika T, Sato S, Uenaka A, Miyata H, Yasuda T, Doki Y, Noguchi Y, Kumon H, Tsuji K, Iwatsuki K, Shiku H, Ritter G, Murphy R, Hoffman E, Old LJ, Monden M, Nakayama E: **Antibody response against NY-ESO-1 in CHP-NY-ESO-1 vaccinated patients.** *Int J Cancer* 2007, **120**:2178–2184.
8. Chen YT, Scanlan MJ, Sahin U, Türeci O, Gure AO, Tsang S, Williamson B, Stockert E, Pfreundschuh M, Old LJ: **A testicular antigen aberrantly expressed in human cancers detected by autologous antibody screening.** *Proc Natl Acad Sci U S A* 1997, **94**:1914–1918.
9. Jungbluth AA, Chen YT, Stockert E, Busam KJ, Kolb D, Iversen K, Coplan K, Williamson B, Altorki N, Old LJ: **Immunohistochemical analysis of NY-ESO-1 antigen expression in normal and malignant human tissues.** *Int J Cancer* 2001, **92**:856–860.
10. Davis ID, Chen W, Jackson H, Parente P, Shackleton M, Hopkins W, Chen Q, Dimopoulos N, Luke T, Murphy R, Scott AM, Maraskovsky E, McArthur G, MacGregor D, Sturrock S, Tai TY, Green S, Cuthbertson A, Maher D, Miloradovic L, Mitchell SV, Ritter G, Jungbluth AA, Chen YT, Gnjatic S, Hoffman EW, Old LJ, Cebon JS: **Recombinant NY-ESO-1 protein with ISCOMATRIX adjuvant induces broad integrated antibody and CD4(+) and CD8(+) T cell responses in humans.** *Proc Natl Acad Sci U S A* 2004, **101**:10697–10702.
11. Eisenhauer EA, Therasse P, Bogaerts J, Schwartz LH, Sargent D, Ford R, Dancey J, Arbuck S, Gwyther S, Mooney M, Rubinstein L, Shankar L, Dodd L, Kaplan R, Lacombe D, Verweij J: **New response evaluation criteria in solid tumours: revised RECIST guideline (version 1.1).** *Eur J Cancer* 2009, **45**:228–247.
12. Wolchok JD, Hoos A, O'Day S, Weber JS, Hamid O, Lebbé C, Maio M, Binder M, Bohnsack O, Nichol G, Humphrey R, Hodi FS: **Guidelines for the evaluation of immune therapy activity in solid tumors: immune-related response criteria.** *Clin Cancer Res* 2009, **15**:7412–7420.
13. Trotti A, Colevas AD, Setser A, Rusch V, Jaques D, Budach V, Langer C, Murphy B, Cumberlin R, Coleman CN, Rubin P: **CTCAE v3.0: development of a comprehensive grading system for the adverse effects of cancer treatment.** *Semin Radiat Oncol* 2003, **13**:176–181.
14. Fujita S, Wada H, Jungbluth AA, Sato S, Nakata T, Noguchi Y, Doki Y, Yasui M, Sugita Y, Yasuda T, Yano M, Ono T, Chen YT, Higashiyama M, Gnjatic S, Old LJ, Nakayama E, Monden M: **NY-ESO-1 expression and immunogenicity in esophageal cancer.** *Clin Cancer Res* 2004, **10**:6551–6558.
15. Stockert E, Jäger E, Chen YT, Scanlan MJ, Gout I, Karbach J, Arand M, Knuth A, Old LJ: **A survey of the humoral immune response of cancer patients to a panel of human tumor antigens.** *J Exp Med* 1998, **187**:1349–1354.
16. Aoki M, Ueda S, Nishikawa H, Kitano S, Hirayama M, Ikeda H, Toyoda H, Tanaka K, Kanai M, Takabayashi A, Imai H, Shiraishi T, Sato E, Wada H, Nakayama E, Takei Y, Katayama N, Shiku H, Kageyama S: **Antibody responses against NY-ESO-1 and HER2 antigens in patients vaccinated with combinations of cholesteryl pullulan (CHP)-NY-ESO-1 and CHP-HER2 with OK-432.** *Vaccine* 2009, **27**:6854–6861.
17. Adams S, O'Neill DW, Nonaka D, Hardin E, Chiriboga L, Siu K, Cruz CM, Angiulli A, Angiulli F, Ritter E, Holman RM, Shapiro RL, Berman RS, Berner N, Shao Y, Manches O, Pan L, Venhaus RR, Hoffman EW, Jungbluth A, Gnjatic S, Old L, Pavlick AC, Bhardwaj N: **Immunization of malignant melanoma patients with full-length NY-ESO-1 protein using TLR7 agonist imiquimod as vaccine adjuvant.** *J Immunol* 2008, **181**:776–784.
18. Valmori D, Souleimanian NE, Tosello V, Bhardwaj N, Adams S, O'Neill D, Pavlick A, Escalon JB, Cruz CM, Angiulli A, Angiulli F, Mears G, *et al*: **Vaccination with NY-ESO-1 protein and CpG in Montanide induces integrated antibody/Th1 responses and CD8 T cells through cross-priming.** *Proc Natl Acad Sci U S A* 2007, **104**:8947–8952.
19. Odunsi K, Matsuzaki J, Karbach J, Neumann A, Mhawech-Fauceglia P, Miller A, Beck A, Morrison CD, Ritter G, Godoy H, Lele S, Dupont N, *et al*: **Efficacy**

of vaccination with recombinant vaccinia and fowlpox vectors expressing NY-ESO-1 antigen in ovarian cancer and melanoma patients. *Proc Natl Acad Sci U S A* 2012, **109**:5797–5802.

20. Sabbatini P, Tsuji T, Ferran L, Ritter E, Sedrak C, Tuballes K, Jungbluth AA, Ritter G, Aghajanian C, Bell-McGuinn K, Hensley ML, Konner J, *et al*: **Phase I trial of overlapping long peptides from a tumor self-antigen and poly-ICLC shows rapid induction of integrated immune response in ovarian cancer patients.** *Clin Cancer Res* 2012, **18**:6497–6508.
21. Small EJ, Schellhammer PF, Higano CS, Redfern CH, Nemunaitis JJ, Valone FH, Verjee SS, Jones LA, Hershberg RM: **Placebo-controlled phase III trial of immunologic therapy with Sipuleucel-T (APC8015) in patients with metastatic, asymptomatic hormone refractory prostate cancer.** *J Clin Oncol* 2006, **24**:3089–3094.

doi:10.1186/1479-5876-11-246
**Cite this article as:** Kageyama *et al.*: Dose-dependent effects of NY-ESO -1 protein vaccine complexed with cholesteryl pullulan (CHP-NY-ESO-1) on immune responses and survival benefits of esophageal cancer patients. *Journal of Translational Medicine* 2013 11:246.